

Piecewise Affine (PWA) Modeling and Switched Damping Control of Two-Inertia Systems with Backlash

Shota Yamada

The University of Tokyo

Chiba, Japan

yamada.shota13@ae.k.u-tokyo.ac.jp

Michael Ruderman

University of Agder

Grimstad, Norway

michael.ruderman@uia.no

Hiroshi Fujimoto

The University of Tokyo

Chiba, Japan

fujimoto@k.u-tokyo.ac.jp

Abstract—Backlash degrades positioning accuracy and can induce mechanical wear and breakage by collisions. Therefore, a lot of studies have been conducted on backlash compensation. The simplest control method for the impact attenuation is torsional damping addition by feedback of torsional velocity. This paper reveals the advantages and disadvantages of the torsional damping addition. Based on the analyses, a novel switched damping control is proposed to realize the responses with smaller overshoot while attenuating the impact. The mechanical system and the proposed controller are described as piecewise affine systems for analyses. The performance of the proposed method is compared with a linear damping control method in simulations and experiments.

Index Terms—Backlash, load-side encoder, piecewise affine system, switching system, two-inertia system

I. INTRODUCTION

In controlling geared mechanical systems, backlash is one of the most important nonlinearities that degrade control performance. Backlash can degrade the accuracy of the load-side positioning, generate limit cycles, and induce mechanical wear and breakage by large impacts caused by collisions between the driving (motor) and driven (load) sides. Since backlash has nondifferentiable property denoted "hard" nonlinearity, it is not easy to compensate effectively.

A lot of studies have been conducted on backlash compensation [1], [2]. Geared mechanical systems are often simplified and modeled as two-mass/inertia systems with backlash. In [1] the compensation methods are divided into two groups. The first one is "strong" action group which moves the motor side quickly [3]. One of the strong compensation methods is an inverse model compensation of the backlash model, but it requires large peak in the motor torque and induces mechanical wear by large impacts caused by collisions. The second one is "weak" action group, which includes gear torque compensation [4], [5], switching control [6], and model predictive control (MPC) [7], [8], etc.

Among the backlash compensation methods, MPC is studied intensively these days due to the several reasons. The first reason is that MPC can deal with the plant model with backlash directly by hybrid system modeling. Two-inertia systems with backlash can be modeled as piecewise affine (PWA) systems

as described in Section II. Though it is not easy to apply MPC to the motion control of mechanical systems due to low sampling times of control systems, MPC for PWA systems can be calculated offline for a given set of states, which is called Explicit MPC [7]. The second reason is that MPC can reduce the impact torque by collisions by constraining and penalizing the torsional velocity (the difference of the motor- and load-sides velocities) within backlash [7], [8]. However, Explicit MPC for PWA systems still need large computation sources. Therefore, we are striving to develop a simple and industrial-oriented control algorithm, which is intuitive and easy to tune, for motion control applications.

The simplest control method for the impact attenuation of the collisions is torsional damping addition by feedback of torsional velocity. This paper reveals the advantages and disadvantages of the torsional damping addition. By the detailed analyses of how the added torsional damping works, a novel switched damping control is proposed to overcome the disadvantage while holding the advantage. The proposed method shows the responses with smaller overshoot while attenuating the impact. The plant model of the two-inertia system with backlash and the switched damping controller are described as PWA systems, and the stability analyses are conducted in PWA framework. The performance of the proposed method is compared with a linear damping (not switching) control method in simulations and experiments.

II. TWO-INERTIA SYSTEM WITH BACKLASH

A. Modeling of two-inertia system with backlash

Several models of two-inertia systems with backlash have already been proposed. The physically reasoned model denoted as "exact model" by introducing a state of the angle between backlash has been proposed in [9]. Though several studies (e.g. [7] and [8]) have used the exact model, in [6] it is stated that the dynamics of the introduced state can be neglected in the practical applications. Since our simulation studies also confirmed that the effect can be neglected, this paper also uses an alternative approach of the deadzone and linear damping model for the modeling of a two-inertia system with backlash.

Equation of motion of a two-inertia system with deadzone and linear damping are expressed as follows:

$$\begin{cases} J_M \dot{\omega}_M + D_M \omega_M = T_M - T_s, & (1) \\ J_L \dot{\omega}_L + D_L \omega_L = T_s + d_L, & (2) \\ \theta_B = \theta_M - \theta_L, & (3) \\ \omega_B = \omega_M - \omega_L, & (4) \end{cases}$$

$$T_s = \begin{cases} 0, & \text{if } |\theta_B| < \beta, \quad i = 0, \\ D_B \omega_B + K(\theta_B - \beta), & \text{if } \theta_B \geq \beta, \quad i = 1, \\ D_B \omega_B + K(\theta_B + \beta), & \text{if } \theta_B \leq -\beta, \quad i = 2. \end{cases} \quad (5)$$

The definition of the variables is given in Table I. Subscripts M , L , and B indicate the motor-side, load-side, and backlash related quantities, respectively. We call the cases $i = 0$ as Backlash mode, $i = 1$ as Positive contact mode, $i = 2$ as Negative contact mode, respectively.

B. Piecewise affine model

By modeling the system as a PWA system, the well-established theories can be employed (see e.g. in [10], [11]). In this paper, PWA system of the below form are considered

$$\dot{x} = A_i x + a_i + B u, \quad \forall x \in X_i, \quad (6)$$

$$G_i x + g_i \geq 0, \quad x \in X_i \quad i \in I, \quad (7)$$

$$F_i x + f_i = F_j x + f_j, \quad x \in X_i \cap X_j \quad i, j \in I. \quad (8)$$

Here, (6) indicates differential equations holding in the separated state space $\forall x \in X_i$. u indicates input and a_i is affine term. $\{X_i\}_{i \in I} \subseteq \mathbf{R}^4$ is a partition of the state space into closed polyhedral cells with pairwise disjoint interior. The index set of the cells is denoted I . The inequalities (7) indicate the partitions of the state space. The equations (8) indicate the boundaries of the jointed two cells of the state space.

Then, the system expressed in (1)–(5) is rewritten in a PWA notation as follows

$$A_0 = \begin{bmatrix} -\frac{D_L}{J_L} & 0 & 0 & 0 \\ -\frac{D_M}{J_M} + \frac{D_L}{J_L} & -\frac{D_M}{J_M} & 0 & 0 \\ 1 & 0 & 0 & 0 \\ 0 & 1 & 0 & 0 \end{bmatrix}, \quad a_0 = \begin{bmatrix} 0 \\ 0 \\ 0 \\ 0 \end{bmatrix}, \quad (9)$$

$$G_0 = \begin{bmatrix} 0 & 0 & 0 & 1 \\ 0 & 0 & 0 & -1 \end{bmatrix}, \quad g_0 = \begin{bmatrix} \beta \\ \beta \end{bmatrix}, \quad (10)$$

$$F_0 = \begin{bmatrix} 0 & 0 & 0 & 1 \end{bmatrix}, \quad f_0 = 0, \quad (11)$$

$$A_1 = \begin{bmatrix} -\frac{D_L}{J_L} & \frac{D_B}{J_B} & 0 & \frac{K}{J_L} \\ -\frac{D_M}{J_M} + \frac{D_L}{J_L} & -\frac{D_M}{J_M} - \frac{D_B}{J_M} - \frac{D_B}{J_L} & 0 & -\frac{K}{J_M} - \frac{K}{J_L} \\ 1 & 0 & 0 & 0 \\ 0 & 1 & 0 & 0 \end{bmatrix}, \quad (12)$$

$$a_1 = \begin{bmatrix} -\frac{K\beta}{J_L} & \frac{K\beta}{J_M} + \frac{K\beta}{J_L} & 0 & 0 \end{bmatrix}^T, \quad (13)$$

$$G_1 = \begin{bmatrix} 0 & 0 & 0 & 1 \end{bmatrix}, \quad g_1 = -\beta, \quad (14)$$

$$F_1 = \begin{bmatrix} 0 & 0 & 0 & 0 \end{bmatrix}, \quad f_1 = \beta, \quad (15)$$

TABLE I
DEFINITION OF PLANT PARAMETERS.

Inertia moment	J	Motor torque	T_M
Viscosity coefficient	D	Joint torque	T_s
Torsional rigidity	K	Torsional damping	D_B
Angle	θ	Angular velocity	ω
Torsional angle	θ_B	Torsional angular velocity	ω_B
Deadzone width	β	Load-side disturbance	d_L

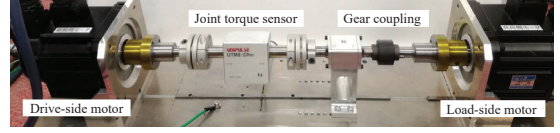


Fig. 1. Outlook of the two-inertia system motor bench.

$$A_2 = A_1, \quad a_2 = -a_1, \quad (16)$$

$$G_2 = -G_1, \quad g_2 = g_1, \quad (17)$$

$$F_2 = F_1, \quad f_2 = -f_1, \quad (18)$$

$$x = \begin{bmatrix} \omega_L \\ \omega_B \\ \theta_L \\ \theta_B \end{bmatrix}, \quad B = \begin{bmatrix} 0 & \frac{1}{J_L} \\ \frac{1}{J_M} & -\frac{1}{J_L} \\ 0 & 0 \\ 0 & 0 \end{bmatrix}, \quad u = \begin{bmatrix} T_M \\ d_L \end{bmatrix}. \quad (19)$$

C. Experimental setup

A motor bench shown in Fig. 1 is used as a setup for a two-inertia system with backlash. The setup consists of two motors with 20-bit encoders, a joint torque sensor, and a gear coupling. These days, the control methods using load-side encoder are gaining a lot of attentions, and our research group has proposed a novel structure with load-side encoder for industrial robots' application in [12]. Based on the industrial trend that the number of load-side encoders is increasing, we assume that load-side encoder of the load-side motor can be used for feedback control. The joint torque sensor is used for the measurement of the impact torque caused by backlash. Backlash is introduced by the equipped gear coupling. The parameters of the setup are identified by frequency responses measurements and shown in Table II. Backlash is measured by motor- and load- sides encoders inputting small-amplitude and low-frequent sinusoidal motor torque. The measurement in Fig. 2 shows that the half backlash width β is identified to be 7.80 mrad.

III. DAMPING CONTROL OF TWO-INERTIA SYSTEM WITH BACKLASH

Torsional damping addition control is widely known as one of the effective control methods for a two-inertia system without backlash. Hung in [13] has revealed that the mechanical systems with transmission elasticities behave similarly to the rigid body by torsional damping addition. The vibration caused by the transmission elasticity can be effectively damped. As for a two-inertia system with backlash, the studies on MPC often

TABLE II
PARAMETERS OF THE TWO-INERTIA SYSTEM MOTOR BENCH.

Motor-side moment of inertia J_M	8.78e-4	kgm ²
Motor-side viscosity coefficient D_M	9.30e-2	Nms/rad
Torsional rigidity K	3.00e2	Nm/rad
Torsional damping D_B	1.00e-1	Nms/rad
Load-side moment of inertia J_L	8.78e-4	kgm ²
Load-side viscosity coefficient D_L	3.60e-2	Nms/rad
Deadzone width β	7.80e-3	rad

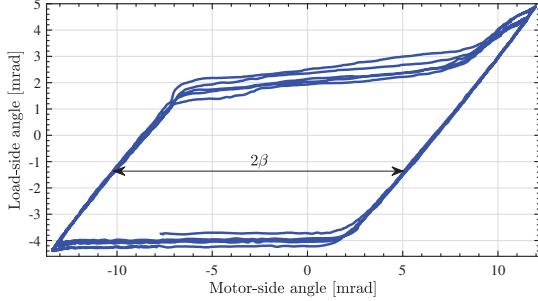


Fig. 2. Backlash identification measurements by using both motor- and load-side encoders at low dynamics conditions.

add damping to the torsional part by constraining or penalizing the torsional velocity term (see e.g. [7] and [8]). This is for avoiding the mechanical wear and breakage by reducing the impact torque and the number of rebounds. However, MPC needs large computation and MPC is challenging to be implemented in standard motion control applications. Though the studies in [7] and [8] try to reduce the computation costs by partially calculating in offline, they still need large computation sources. Therefore, our approach is to develop a simple control algorithm, which is intuitive and easy to tune in applications.

A. Load-side position controller

Damping addition controller is implemented in inner loop with a load-side position controller in outer loop. In this paper, PD controller is applied for positioning as a widely used technique. The motor torque T_M is calculated as follows

$$T_M = T_{PD} + T_B, \quad (20)$$

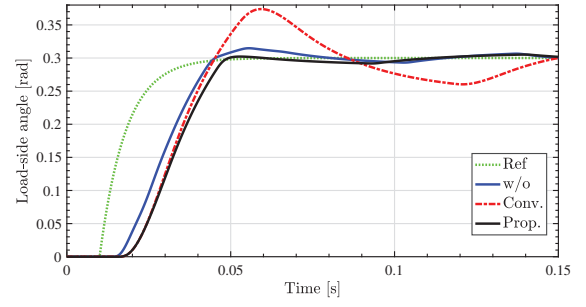
$$T_{PD} = \left(K_P + \frac{K_D s}{1 + \tau_{DL} s} \right) (\theta_{Lref} - \theta_L), \quad (21)$$

$$T_B = K_B \omega_B. \quad (22)$$

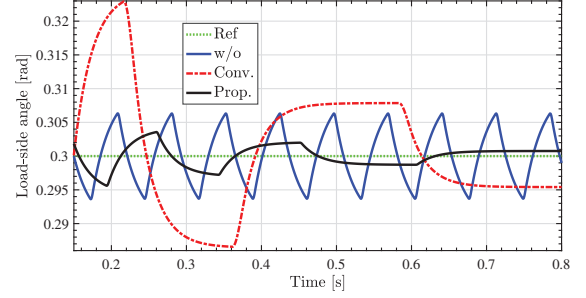
The control efforts by PD controller T_{PD} and damping controller T_B are expressed in (21) and (22), respectively. Here, θ_{Lref} is a reference value of the load-side angle.

B. Linear damping control (Conventional method)

The simplest control method for torsional damping addition is a feedback of torsional velocity with gain K_B as already shown in (22). The negative gain K_B attenuates the impact torque by adding the linear damping, but the added damping delays the rising time simultaneously. There is a trade-off



(a) The responses around the rising phase.



(b) The responses around the settling phase.

Fig. 3. Step responses of the load-side angle.

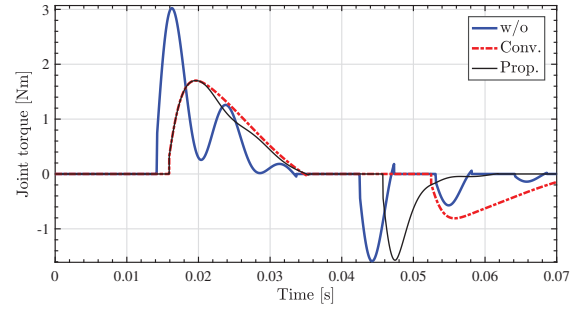
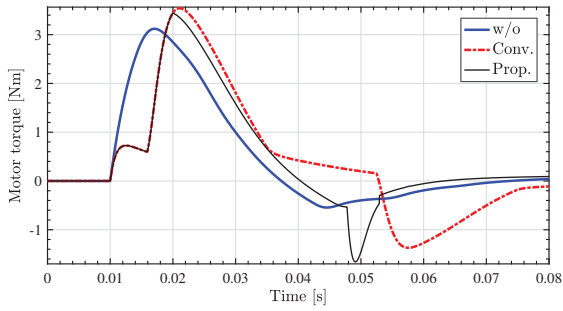


Fig. 4. The impact torque comparison when step reference of the load-side angle is input.

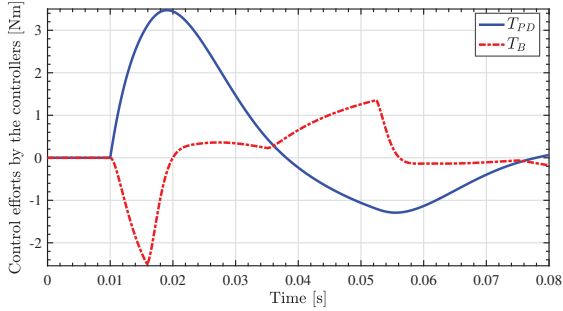
between the impact attenuation and the fast responses when designing. The gain should be designed by considering the allowable impact torque of the mechanical system.

To confirm the impact attenuation effect, simulation is conducted using the plant introduced in Section II. The gains of PD controller are designed by the pole placement method to achieve sufficient fast response, and then the gain K_B is designed to reduce the impact torque. The gains of PD controllers are designed such that their closed poles are placed to be $(s + \omega_1)(s^2 + 2\zeta\omega_2 s + \omega_2^2)$, $\omega_1 = 2\pi \cdot 18$, $\omega_2 = 2\pi \cdot 15$, and $\zeta = 0.70$ assuming the plant model is rigid body. K_B is designed to be -0.80 . The value of the controller parameters in the all control methods are the same for the sake of a fair comparison.

Figures 3 and 4 show the responses of the load-side angle and the joint torque when the 0.30 rad step reference is given for the load-side angle at 0.010 s. Step reference indicated by



(a) Motor torque responses comparison.



(b) Details of the control efforts in Conventional method.

Fig. 5. Motor torque responses when step reference of the load-side angle is input.

the green dotted line is filtered with the first order low-pass filter whose cutoff frequency is 20 Hz. Initial position of the motor side is at the middle of the deadzone. The blue solid line indicates the response without inner damping controller, that is, $K_B = 0$, while the red dashed line indicates the response with linear damping controller. Figure 3(a) shows that the load-side angle responses around rising phase. As expected, with damping control, the transient responses are delayed a little compared to the responses without damping control. On the other hand, the impact torque is attenuated by damping addition as shown in Fig. 4. In this case, 44% of the first impact torque is reduced. Also, Fig. 3(b) shows that stable limit cycle is induced in the response without damping while not seen in Conventional method thanks to the damping addition.

However, Fig. 3(a) shows that the response with damping controller has larger overshoot, and thus results in larger vibration also in settling phase as shown in Fig. 3(b). The reason why the larger overshoot is caused by damping addition is revealed by analyzing the behavior of the motor- and load-sides. Firstly, the motor side in backlash is accelerated and has the collision with the load side. In this acceleration phase, the linear damping should be added for the impact attenuation. After small rebounds, the load side is required to decelerate for settling. In this deceleration phase, the motor side moves from the positive contact state to the negative contact state. With the added damping, this motor-side traversal motion is delayed, and the load side has more time to move. Thus, larger overshoot is caused by damping addition.

The above consideration is confirmed by analyzing the motor torque responses. Figure 5(a) shows that the comparison of the motor torque responses, and Fig. 5(b) shows the respective control efforts (T_{PD} and T_B) in Conventional method. Figure 5 indicates that the linear damping controller decreases the motor torque at the rising phase, and increases the motor torque at the braking phase starting from about 0.035 s. The increase of the motor torque at the braking phase leads the slow traversal motion of the motor side. In this way, linear damping addition generates large overshoot, though it can reduce the impact torque. Switched damping control method is proposed to solve this trade-off.

C. Switched damping control (Proposed method)

1) *Switching condition*: The above analyses indicate that linear damping is required in acceleration phase for impact attenuation, but not required in deceleration phase for avoiding large overshoot. When the direction of the motion is negative, linear damping is required in deceleration phase, but not required in acceleration phase. To realize these two demands, switched damping control is proposed.

Proposed method switches the gain K_B according to the state variables as follows

$$K_B = \begin{cases} \text{const} < 0, & \text{if } \omega_B * \omega_L \geq 0 \\ 0, & \text{else.} \end{cases} \quad (23)$$

The switching condition can be equally converted to $(0 \leq \omega_L \leq \omega_M) \vee (\omega_M \leq \omega_L \leq 0)$ for additional interpretation. The switching is done based on the plant's state variables to include the closed-loop system into PWA frame. The switching condition indicates that when the directions of the motor- and load-sides velocities are same and the motor-side velocity is faster than the load-side velocity, the damping is added, and otherwise not. In this way, the acceleration phase is approximately expressed by the condition only using the plant's state variables.

It is confirmed by numerous simulations that the switching condition works correctly both in target value responses and load-side disturbance responses. For example, the disturbance responses are considered. When the load-side disturbance is input, the two-inertia system is either in backlash mode or in contact mode. When the system is in backlash mode, the load-side disturbance makes the load side faster than the motor side. In this case, there should not be damping because the motor side should have the contact with the load side as soon as possible for disturbance suppression. Therefore, Proposed method has better performance than Conventional method. When the system is in positive contact mode, the positive disturbance makes the load side faster than the motor side. In this case, there should not be damping, and the condition works correctly. When the negative disturbance is input, the velocities become to $\omega_M \leq \omega_L \leq 0$. In this case, there should be damping because the motor side should not move away to have the contact with the load side as soon as possible for disturbance suppression. Thus, Proposed method shows better performance than the method without damping.

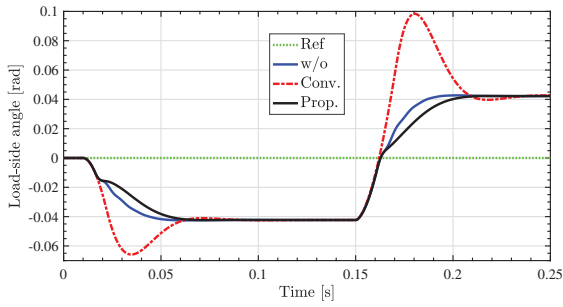


Fig. 6. The load-side angle responses comparison when step load-side disturbances are input -0.50 Nm at 0.010 s and 1.0 Nm at 0.15 s.

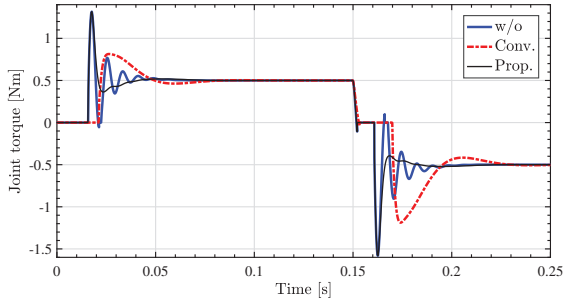
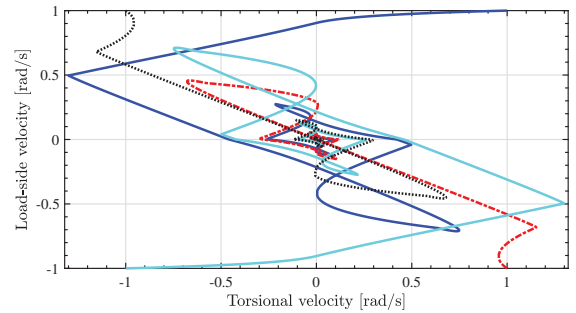


Fig. 7. The impact torque comparison when step load-side disturbances are input -0.50 Nm at 0.010 s and 1.0 Nm at 0.15 s.

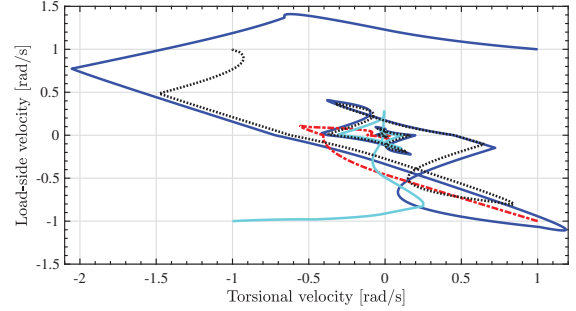
The switching condition does not perform efficiently in some cases, e.g. in the rebounding and releasing phase after the impacts, the motor-side velocity becomes smaller than the load-side velocity, that is, the damping controller does not work. In the phase, there should be damping because the motor side should not move away to have a contact as soon as possible to accelerate/decelerate the load side in positive/negative direction motion. However, in most cases the switching condition performs appropriately.

2) *Simulation evaluation of Proposed method:* The advantages of Proposed control method are shown in Figs. 3 and 4. In Fig. 3, Proposed method shows almost same size of the overshoot as the method without damping while the impact torque is much smaller.

Figures 6 and 7 show the load-side angle responses and the joint torque responses when step load-side disturbances are input -0.50 Nm at 0.010 s and 1.0 Nm at 0.15 s. Initial condition is that both motor- and load- sides are not moving and the motor-side is at the middle of the deadzone. The angle response in Conventional method in red dashed line shows less disturbance suppression performance since the damping makes the motor side move away from the load side. The joint torque responses shown in Fig. 7 indicate that the impact torque is reduced in Conventional method but not reduced in Proposed method. For disturbance suppression, damping should not be added to have the contacts between the motor and load sides as soon as possible in terms of controllability of the load side. Therefore, Proposed method shows better performance



(a) Free responses in backlash mode.



(b) Free responses in contact mode.

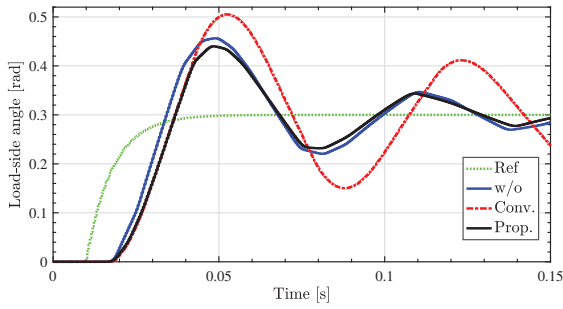
Fig. 8. Typical trajectories for stability analyses.

than Conventional method. Moreover, Proposed method shows better performance than the method without damping, since after the impact, the motor-side velocity becomes larger than the load-side velocity and the damping controller works not to move the motor side away from the load side.

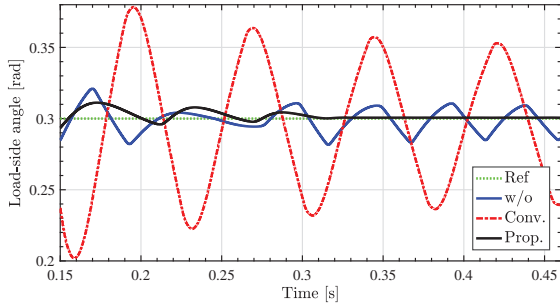
3) *Stability analyses:* Stability is analyzed by using the PWA systems notation. The closed-loop system with Proposed method consists of the state space divided into 12 cells since the plant has 3 cells about θ_B and the switched damping controller has 4 cells about ω_L and ω_B . Since the positive contact mode and the negative contact mode in (5) have the symmetrical dynamics, it is enough to consider two cases: backlash mode and contact mode, which results in considering 8 cells in total. Though there are toolboxes for finding Lyapunov function for stability analyses (e.g. [14]), it was not possible to find a suitable Lyapunov function candidate for our closed-loop systems with internal deadzone nonlinearity and switching control, both in PWA notation. Therefore, the stability is analyzed by seeing the convergence of the typical trajectories starting from different 8 cells. Figure 8(a) shows the free responses in backlash mode ($\theta_B=0$ rad) with four cases of initial conditions: $(\omega_B$ [rad/s], ω_L [rad/s])=(1.0, 1.0), (1.0, -1.0), (-1.0, -1.0), (-1.0, 1.0). Figure 8(b) shows the free responses in contact mode ($\theta_B=0.010$ rad) with the four cases. Figure 8 indicate the convergence of the typical trajectories starting from different 8 cells.

IV. EXPERIMENTS

The controller parameters are set to be the same as those in the simulations, and controllers are discretized by Tustin



(a) The responses around the rising phase.



(b) The responses around the settling phase.

Fig. 9. Step responses of the load-side angle in the experiments.

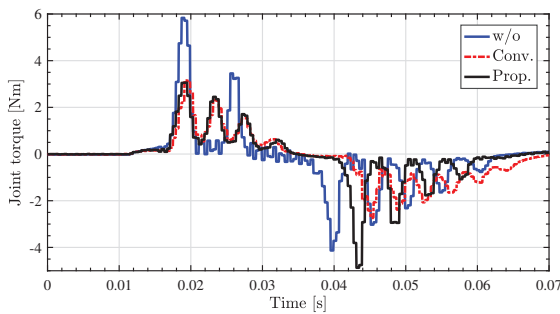


Fig. 10. The impact torque comparison when step reference of the load-side angle is input in the experiments.

conversion and implemented with the sampling frequency of 2.5 kHz. Initial position is set at the middle point of the backlash by the motor-side position controller.

Figures 9 and 10 show the load-side angle responses and the joint torque responses in the experiments, respectively. They show the similar tendency to the simulation ones shown in Figs. 3 and 4. The amplitude of overshoot is different between Fig. 3 and Fig. 9(a) due to the modeling errors such as parameter identification error and unmodeled nonlinear friction. Figure 9(a) indicates that the Conventional method shows the delayed transient responses with larger overshoot compared to the method without damping. The Proposed method shows better settling response as shown in Fig. 9(b). The first impact torque is reduced by damping addition as shown in Fig. 10. As for the second impact in braking phase, Conventional method reduces the impact torque with added

damping but this generates large overshoot as discussed in Section III. Proposed method does not attenuate the second impact, which indicates that the switching condition works correctly.

V. CONCLUSION

Torsional damping addition can attenuate impacts by backlash, but it simultaneously deteriorates the transient responses of the load-side position. To solve this trade-off, the effect of the torsional damping addition is analyzed, and the switched damping control method is proposed. Proposed method shows the responses without large overshoot while attenuating the impact torque in the simulations and the experiments. The local stability is analyzed in the phase-plane while the whole system description is provided by using the PWA formalism.

VI. ACKNOWLEDGEMENT

This work has received funding from the European union Horizon 2020 research and innovation program H2020-MSCA-RISE-2016 under the grant agreement No. 734832.

REFERENCES

- [1] M. Nordin and P. Gutman: "Controlling mechanical systems with backlash - a survey", *Automatica*, 38, pp. 1633–1649, Oct. 2002.
- [2] I. Ponce, Y. Orlov, L. Aguilar, and J. Alvarez: "Nonsmooth H_∞ synthesis of non-minimum-phase servo-systems with backlash", *Control Engineering Practice*, vol. 46, pp. 77–84, Jan. 2016.
- [3] A. Azenha and J. A. T. Machado: "Variable structure control of robots with nonlinear friction and backlash at the joints", *Proc. IEEE Int. Conf. Robotics and Automation*, pp. 366–371, Apr. 1996.
- [4] M. Odai and Y. Hori: "Speed control of 2-inertia system with gear backlash using gear torque compensator", *IEEE Int. Workshop Adv. Motion Control*, pp. 234–239, Jun./Jul. 1998.
- [5] M. Yang, D. Xu, W. Zheng, and X. Lang: "Shaft Torque Limiting Control Using Shaft Torque Compensator for Two-Inertia Elastic System With Backlash", *IEEE/ASME Trans. Mechatronics*, vol. 21, no. 6, pp. 2902–2911, Dec. 2016.
- [6] A. Formentini, A. Oliveri, M. Marchesoni, and M. Storaice: "A Switched Predictive Controller for an Electrical Powertrain System With Backlash", *IEEE Trans. Power Electron.*, vol. 32, no. 5, pp. 4036–4047, May. 2017.
- [7] P. Rostalski, T. Besselmann, M. Baric, F. Van Belzen, and M. Morari: "A hybrid approach to modelling, control and state estimation of mechanical systems with backlash", *Int. Jour. Control*, vol. 80, no. 11, pp. 1729–1740, Nov. 2007.
- [8] Y. Li, A. Hansen, J. Karl Hedrick, and J. Zhang: "A receding horizon sliding control approach for electric powertrains with backlash and flexible half-shafts", *Int. Jour. Vehicle System Dynamics*, pp. 1–19, Jun. 2017.
- [9] M. Nordin, J. Galic, and P. Gutman: "New models for backlash and gear play", *Int. Jour. Adaptive control and signal processing*, vol. 11, no. 1, pp. 49–63, Feb. 1997.
- [10] M. Johansson and A. Rantzer: "Computation of Piecewise Quadratic Lyapunov Functions for Hybrid Systems", *IEEE Trans. Autom. Control*, vol. 43, no. 4, pp. 555–559, Apr. 1998.
- [11] M. Johansson: "Piecewise Linear Control Systems", *Springer*, 2003.
- [12] S. Yamada, K. Inukai, H. Fujimoto, K. Omata, Y. Takeda, and S. Makinouchi: "Joint torque control for two-inertia system with encoders on drive and load sides", *Proc. of the 13th IEEE Int. Conf. Ind. Informat. (INDIN)*, pp. 396–401, Jul. 2015.
- [13] J. Y. Hung: "Control of Industrial Robots that Have Transmission Elasticity", *IEEE Trans. Ind. Electron.*, vol. 38, no. 6, pp. 421–427, Dec. 1991.
- [14] S. Hedlund and M. Johansson: "A toolbox for computational analysis of piecewise linear systems", *Proc. of European Control Conf. (ECC)*, pp. 4578–4583, Aug./Sep. 1999.